Dynamic Behavior and Management Strategy of Hybrid Wind/Fuel Cell System

A. Meharrar[1,*], M. Hatti[2], M. Tioursi[3] and T. Benmessaoud[1]

[1]*Tissemsilt University Center, Sciences and Technology Department, Tissemsilt, Algeria*

[2]*UDES, Solar Equipments Development Unit EPST-CDER. 11th National Road, Bou Ismail, Tipaza, Algeria*

[3]*Faculty of Electrical Engineering, University of Sciences and Technology of Oran, BP 1505, EL M'Naouer, Oran, Algeria*

Abstract: hybrid generation system is considered as a solution for the uncontrolled energy production from such dispersed sources as wind generation. In this paper, modeling and control of wind/FC system is proposed. Dynamics models for the main system components, namely, wind energy conversion system (WECS), fuel cell, electrolyses, power electronic interfacing circuits, hydrogen storage tank and ultra-capacitor are developed. Also, a variable speed wind generation maximum power point tracking (MPPT) based on Adaptative Neuro-Fuzzy Inference system (ANFIS) is presented. Based on the dynamic component model, a simulation model for the proposed hybrid energy system has been developed using Matlab/Simulink and the power flows management strategy are proposed. The result shows that this system can tolerate the rapid changes in wind speed and/or power demand. This results shows also that, the overall power management strategy is effective and the power flows among the different energy sources and the load demand is balanced successfully.

Keywords: Dynamic, Management, Wind power, Fuel cell, Ultra-capacitor, Hybrid power generation, ANFIS.

I. INTRODUCTION

Wind energy is one of world's fastest growing energy technologies. The disadvantage of wind turbine is that naturally variable wind speed causes voltage and power fluctuation problems at the bad side. This problem can be solved by using hybrid generation systems. The significant problem is to store the energy generated by wind turbine for future use when the power demand is greater than the power variable, a conventional batteries or diesel generator have been used as second energy source. These solutions have several disadvantages. The new trend is to use fuel cell based energy sources. This solution provides significant advantages in terms of energy density and long-term storage [1, 2].

Various modeling techniques are developed by researchers to model components of HRES (hybrid renewable energy system). Performance of individual component is either modeled by deterministic or probabilistic approaches [3]. In this paper, a detailed dynamic model, simulation and management of a wind/fuel cell /ultra-capacitor hybrid power generation is developed. The system incorporates a water electrolyzer and storage tank to supply the fuel cell stack with hydrogen.

The dc power required for hydrogen generation is supplied through the dc bus during surplus /wind power. The generated hydrogen is stored in tanks to be utilized by the fuel cells when the wind energy source fails to supply the load demand [4]. The UC bank serves as a short duration power source to meet the excess power that cannot be satisfied by the FC or the wind system.

The wind/FC/ UC hybrid system modeling and simulation are performed using MATALB/SIMULINK.

Simulation results are presented to examine the dynamic performance of the system and its potentiality in autonomous operation.

II. HYBRID WIND/FUEL CELL/ULTRA-CAPACITOR SYSTEM DESCRIPTION AND MODELING

In this section, the dynamic simulation model is described for the wind /FC/UC hybrid generation system. The block diagram of the integrated overall system is shown in Figure **1**. The developed system consists of a horizontal axis wind turbine compiled to a permanent magnet synchronous generator (PMSG), an AC/DC controlled rectifier and FC/UC system with a boost type DC/DC.

The common DC bus collects the total energy from the wind and fuel cell subsystems and uses it partly to charge the UC and partly to generate hydrogen from the electrolyzer.

*Address correspondence to this author at the Tissemsilt University Center, Sciences and Technology Department, Tissemsilt, Algeria;
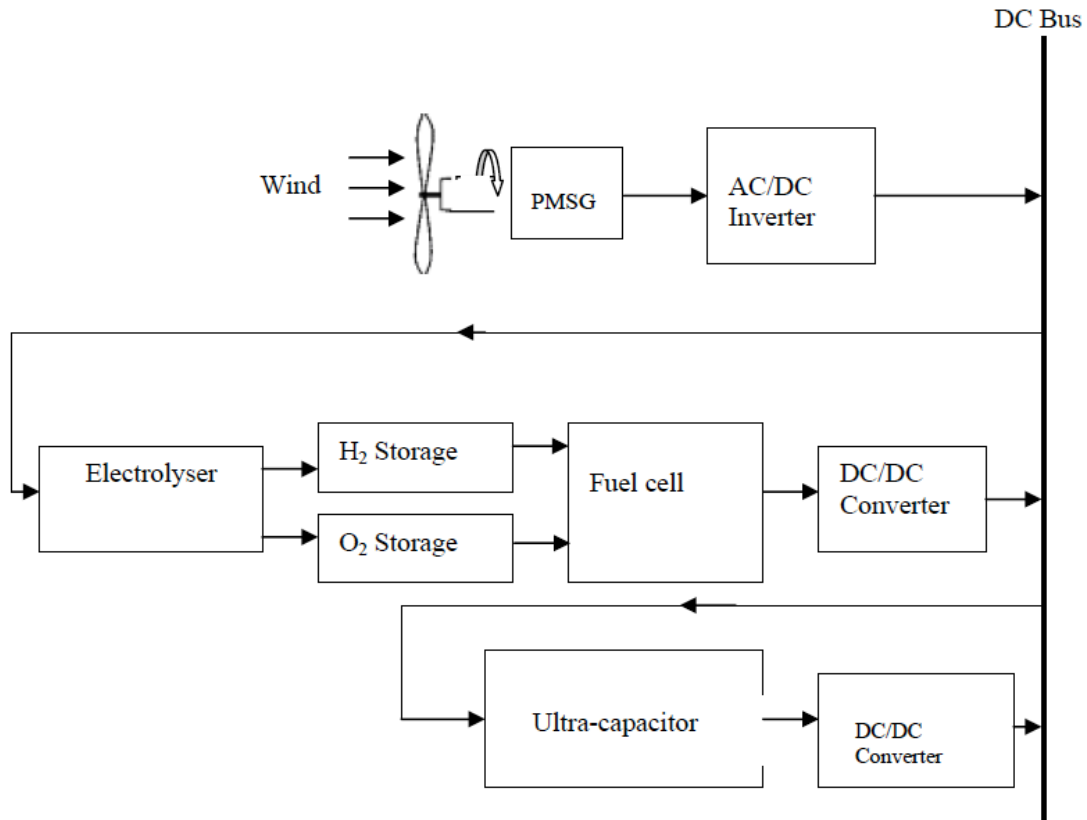Tel: +213552054623; Fax: +21346417377;
E-mail: meharrar_aoued@yahoo.fr

Figure 1: Flow diagram illustrating wind/FC/UC energy-hydrogen storage hybrid power generation system.

III. WIND ENERGY CONVERSION SUBSYSTEM (WECS)

The block diagram of the wind energy system adopted in this paper is shown in Figure **2**. It consists of a horizontal axis wind turbine compiled to a permanent magnet synchronous generator (PMSG). A detailed description of the wind model can be found in [5].
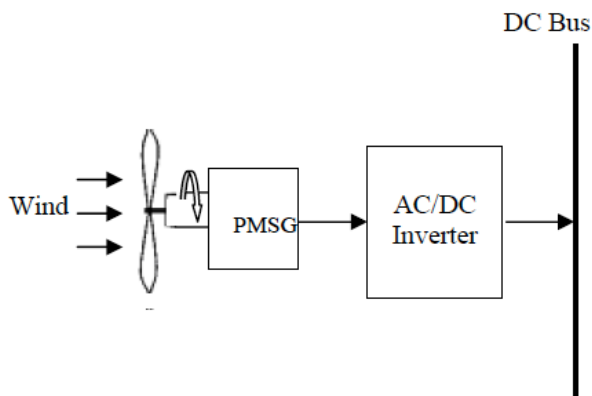

Figure 2: Wind generation system configuration.

The system is designed to achieve maximum power tracking (MPT) and output voltage regulation within a wide range of wind speed variation by means of MPPT block.

IV. WIND TURBINE MODEL

The power extracted from the wind is given by [6]:

$$P_t = \frac{1}{2} c A C_p v^3 \tag{1}$$

Where:

ρ : is the air density in (Kg/m^3).

A: is the area swept by the rotor blades in (m^2).

v: is the wind velocity in (m/s).

Cp: is called the power coefficient or the rotor efficiency and is function of tip speed ration and pitch angle.

The tip speed ration is defined as:

$$\lambda = \frac{\Omega R}{v} \tag{2}$$

Where:

Ω: is the rotational speed of the wind turbine in (rad/s).

R: is the blade radius in (m).

Manufactures usually give an experimental relationship between C_p and λ parameters, for several

values of the rotation speed Ω. In order to evaluate the C_p coefficient, interpolation functions are used to approximate this experimental relationship, within each range of instantaneous values of λ. From this process, the following expressions result:

$$C_p = -v^3(0.12992\lambda^3 - 0.11681\lambda^2 + 0.45406\lambda) \tag{3}$$

The mechanical system is represented by the following equation:

$$J\frac{d\Omega}{dt} = T_m - T_{em} - f\Omega \tag{4}$$

Where:

J: is the total inertia which appears on the shaft of the generator in $(Kg.m^2)$.

T_m: is the mechanical torque in (N.m).

T_{em}: is the electromagnetic torque in (N.m).

Ω: is the rotational speed of the wind turbine in (rad/s).

f: is a viscous friction coefficient in $(N.m.s.rad^{-1})$.

V.   PERMANENT MAGNET SYNCHRONOUS GENERATOR (PMSG)

The space vector theory of the space vector gives the dynamic equation of the stator currents as follows:

$$\frac{dI_{sd}}{dt} = \frac{1}{L_d}(V_{sd} - R_s I_{sd} + p\Omega L_q I_{sq}) \tag{5}$$

$$\frac{dI_{sq}}{dt} = \frac{1}{L_q}(V_{sq} - R_s I_{sq} - pL_{sd}I_{sd}\Omega - p\Omega\Phi_m) \tag{6}$$

Where:

R_s: is the phase resistance of the stator wind in (Ω).

L_d and L_q are the d-q stator inductances respectively in (H).

Φ_m: is the flux of the permanent magnetic in (Wb).

V_{sd} and V_{sq}: are the d-q components of the stator voltage respectively in (V).

I_{sd} and I_{sq}: are the d-q components of the stator currents respectively in (A).

P: is the number of pairs of poles.

The electromagnetic torque is given by:

$$T_{em} = p(\Phi_m I_{sq} + (L_d - L_q)I_{sd}I_{sq}) \tag{7}$$

VI. ANFIS CONTROL OF THE WECS

The WECS includes the wind turbine; the PMSG and the rectifier (Figure **3**). The rectifier makes it possible to control the PMSG flux and consequently the speed of generator. The Block MPPT wind provides the value I_{sqref} corresponding to the value of the reference electromagnetic torque. In this study, the vector control strategy applied to the PMSG, which consists in imposing a reference of the forward current I_{sdref} to zero, is applied [6].
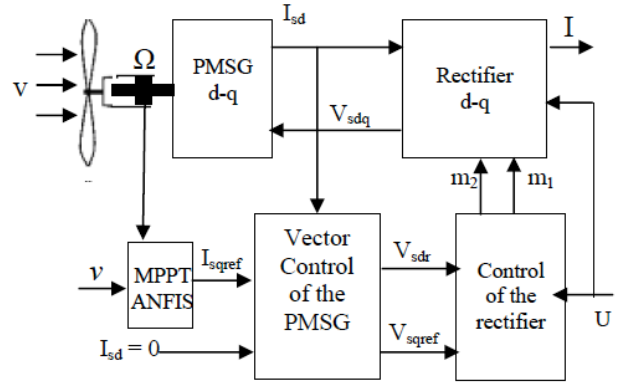

Figure 3: Energetic Macroscopic Representation of the WECS.

From the variation of the wind speed *v*, a Neuro-fuzzy model made up of radial basis functions computes the optimal speed rotation and thus the aerodynamic torque T_{mref}. This computation is based on the mechanical characteristics of the wind turbine. The optimal torque gives the *q*- axis reference current I_{sqref}. The *d*- and *q*- axis reference currents applied to two PI regulators and two decoupling stages give the *d*- and *q*-axis reference voltages V_{sdref} and V_{sqref}. These
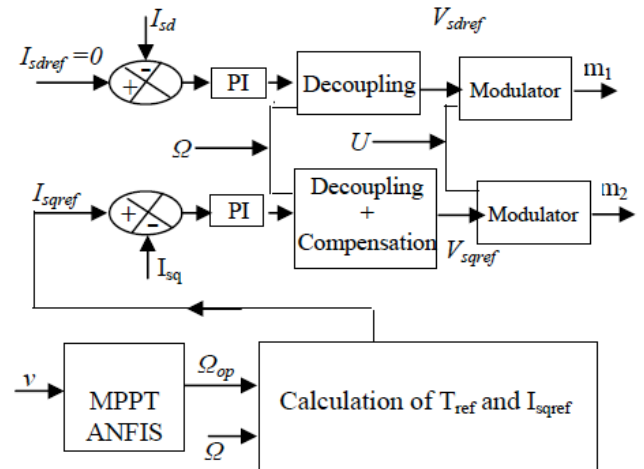

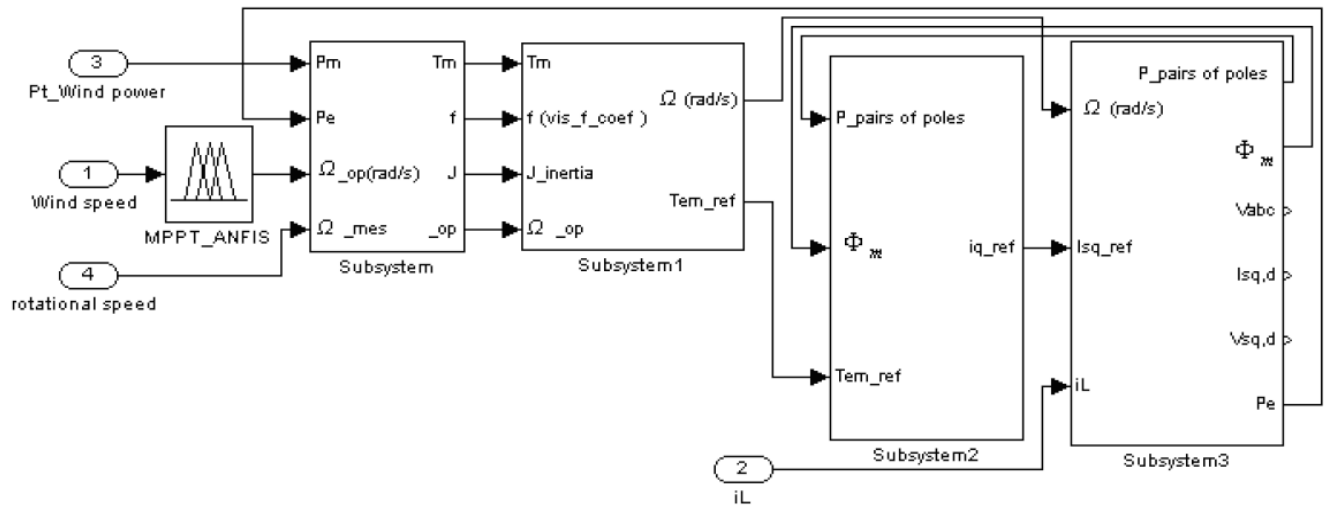**Figure 4:** ANFIS Control of the WECS.

Figure 5: Simulink model of the PMSG.

voltages applied to two modulators provide the switching functions of the rectifier which gives the modulated current I_l. The control strategy of the WECS, previously described, is illustrated in Figure **4**.

The simulation model of the PMSG is illustrated in Figure **5**.

VII. FUEL CELL SUBSYSTEM

The fuel cell, as a renewable energy source, is considered one of the most promising sources of electric power. Fuel cells are not only characterized by higher efficiency than conventional power plants, but they are also environmentally clean, have extremely low emission of oxides of nitrogen and sulfur, and have very low noise [7].

Fuel cells are electrochemical devices that convert the chemical energy of a reaction directly into electrical energy. They have a potential to achieve a level of efficiency beyond 70% when used in a cogeneration facility [8]. Fuel cells are classified by the type of electrolyte used in the cells and include: (1) proton exchange membrane (polymer) electrolyte fuel cell (PEMFC), (2) alkaline fuel cell (AFC), (3) phosphoric acid fuel cell (PAFC), (4) molten carbonate fuel cell (MCFC), and (5) solid oxide fuel cell (SOFC). These fuel cells are listed in the order of approximate operating temperature, ranging from 80°C for PEMFC to1000°C for SOFC [9].

Conventional FC design and the potential to use many fuels including gasoline and diesel without expensive external reformer that create more volatile chemicals [10].

VIII. SOFC MODEL

Many models have been proposed to simulate fuel cells in the literature [11]. The dynamic model of the fuel cell is the electrochemical model with the component material balance equations. The model is also based upon the voltage activation, concentration and Ohmic losses (the Nernst voltage equation) [10].

According to the mathematical model the stack voltage is given as [12, 13]:

$$V_{FC} = N_0 V_0 - rI - \eta_{act} - \eta_{con} \tag{8}$$

$$V_0 = \left(E_0 + \frac{RT}{2F} \ln \frac{P_{H_2} \cdot (P_{O_2})^{0.5}}{P_{H_2O}} \right) \tag{9}$$

Where:

N_0: is the number of cells.

V_0: is the open circuit reversible cell potential,

E_0: is the standard reversible cell potential.

r: ohmic resistance.

η_{ac}: activation losses.

η_{con}: concentration losses.

R: gas constant.

F: is the Faraday's constant.

I: is the stack current.

P_{H_2} : is the hydrogen partial pressure.

P_{O_2} : is the oxygen partial pressure.

P_{H_2} : is the water partial pressure.

Tacking the Laplace transforms, the expression for the hydrogen partial pressure is described as [14, 15]:

$$P_{H_2}(S) = \frac{1/K_{H_2}}{(1 + \tau_{H_2}S)}(q_{H_2}^{in} - 2 \cdot K_r I) \tag{10}$$

Where:

$K_r = \dfrac{N_0}{4F}$: Modeling constant.

K_{H_2} : Hydrogen valve molar constant

τ_{H_2} : Hydrogen time constant

$q_{H_2}^{in}$: Hydrogen input flow.

Similarly, water partial pressure and oxygen partial pressure can be obtained as:

$$P_{H_2O}(S) = \frac{1/K_{H_2O}}{(1 + \tau_{H_2O}S)}(2 \cdot K_r \cdot I) \tag{11}$$

$$P_{O_2}(S) = \frac{1/K_{O_2}}{(1 + \tau_{O_2}S)}(q_{O_2}^{in} - K_r \cdot I) \tag{12}$$

Where:

K_{H_2O} , K_{O_2} : water and oxygen valve molar constant, respectively.

τ_{H_2O} , τ_{O_2} : water and oxygen time constant, respectively.

$q_{O_2}^{in}$: Oxygen input flow.

The fuel cell system consumes hydrogen according to the power demand. The hydrogen is obtained from high-pressure hydrogen tank for stack operation. During operational conditions, to control hydrogen flow rate according to the FC power output, a feedback control strategy is utilized. To achieve this feedback control, FC current from the output is taken back to the input while converting the hydrogen into molar form [16, 17]. The amount of hydrogen available from the hydrogen tank is given by

$$q_{H_2}^{req} = \frac{N_0 \cdot I}{2FU} \tag{13}$$

Where:

$q_{H_2}^{req}$: Amount of hydrogen flow required to meet the load change.

U: Hydrogen utilization.

The hydrogen–oxygen flow ratio $r_{H–O}$ in the FC system determines the oxygen flow rate [18]:
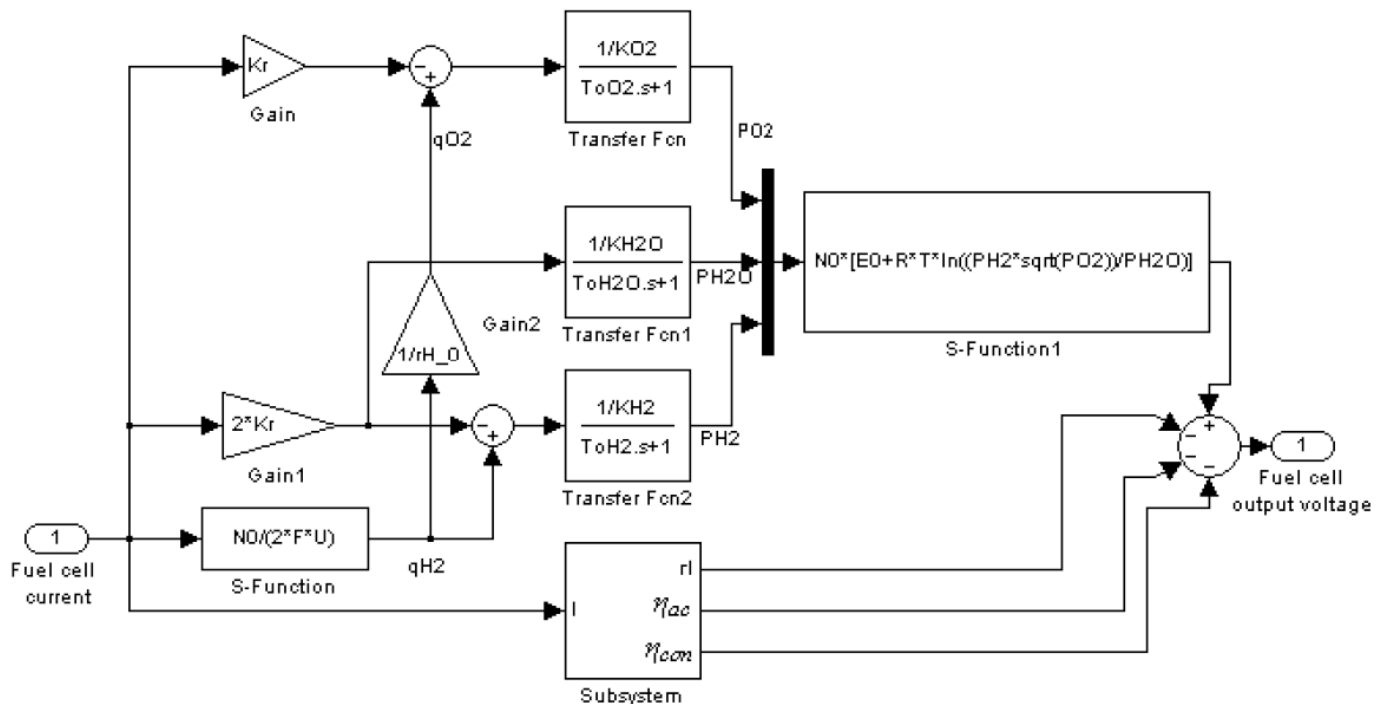

Figure 6: Dynamic model of the FC system.

$$q_{O_2}^{req} = \frac{1}{r_{H\_O}} q_{H_2}^{req} \tag{14}$$

The block diagram of the SOFC model based on the above equations is shown in Figure **6**.

IX. DC/DC BOOST CONVERTER

The main advantages of the boost converter are higher efficiency and reduced component count and it converts the unregulated voltage into desired regulated voltage by varying the duty cycle at high switching frequency lowering the size and cost of energy storage components [19]. The selection of components like boost inductor value and capacitor value is very important to reduce the ripple generation for a given switching frequency. However large inductance tends to increase the start-up time slightly while small inductance allow the coil current to ramp up to higher levels before switch turns off [20]. Figure **7** shows the circuit diagram of a boost DC/DC converter.
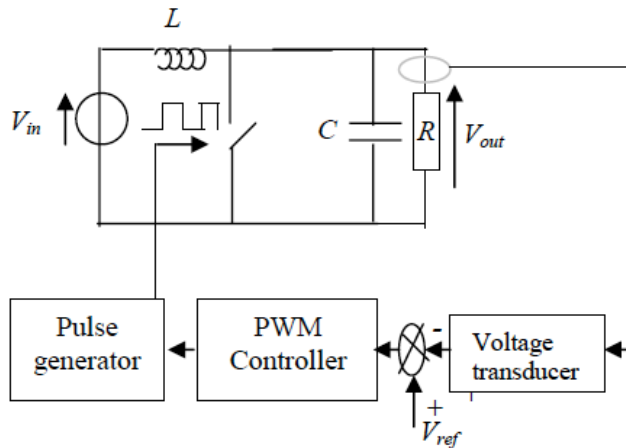

Figure 7: Boost DC/DC converter.

The output voltage regulation feedback is also given in the figure. At steady-state, the average value of the output voltage is given as:

$$V_{out} = \frac{V_{in}}{1 - \alpha} \tag{15}$$

Where α is the duty ratio of the switching pulse.

The controller for the converter is to regulate the DC bus voltage within a desirable range. The output voltage is measured and compared with the reference value. The error signal is processed through the Pulse Width Modulation (PWM) controller, wich can be a simple PI controller, and the output of the controller is used to generate a PWM pulse with the right duty ratio

so that the output voltage follows the reference value [21].

X. ULTRA CAPACITOR BANK

Ultracapacitors or electrochemical double layer capacitors take advantage of the charge stored in their electrochemical double layer and provide high capacities. Thanks to their compacity, ultracapacitors can store an higher amount of energy than conventional capacitors. Moreover, ultracapacitors are currently available on the market with capacitance ranges up to 2700F for a voltage of 2 to 3V; they can release energy at high or low rate [22].

The classical equivalent circuit of the UC unit, shown in Figure **8**, consists of a capacitance (C), an equivalent series resistance (ESR) representing the charging and discharging resistance and an equivalent parallel resistance (EPR) representing the self-discharging losses [23, 24].

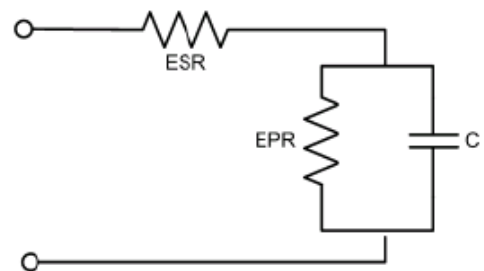The EPR models leakage effects and influences long-term energy storage performance of the UC [25, 26].

Figure 8: Classical equivalent model for the UC unit.

The state of charge of the UC can be described as a percent age of the rated energy capacity, which depends on the terminal output voltage. The energy flowing out from the UC is directly deter mined by the capacitance and the voltage change as expressed in Eq11, [27, 28]

$$E = \frac{1}{2} C(V_i^2 - V_f^2) \tag{16}$$

Where:

V_i: initial voltage.

V_f: final voltage.

The real UC bank can be modeled by using multiple UC cells in parallel and series. The total resistance and capacitance of the UC bank are given by [27]:

$$R_{UCbank} = n_1 \frac{R_{ESR}}{n_2} \tag{17}$$

$$C_{UCbank} = n_2 \frac{C}{n_1} \tag{18}$$

Where:

n_1: number of capacitors in series.

n_2: number of UC branches in parallel.

R_{ESR}: equivalent series resistance.

The state-of-charge (SOC) of the ultracapacitor is defined as:
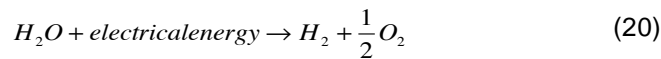
$$SOC = \frac{V_{oc}}{V_{max}} \tag{19}$$

Where:

V_{oc}: is the open-circuit voltage of the ultra-capacitor.

V_{max}: is the maximum open-circuit voltage of the ultra-capacitor at full charge.

XI. ELECTROLYZER MODEL

An electrolyzer is advice that produces hydrogen and oxygen from water. The electrochemical reaction of water electrolysis is given by:

$$H_2O + electrical\,energy \rightarrow H_2 + \frac{1}{2}O_2 \tag{20}$$

There are three principal types of water electrolyser:- alkaline (referring to the nature of its liquid electrolyte), proton-exchange membrane (referring to its solid polymeric electrolyte), and solid-oxide (referring to its solid ceramic electrolyte). The alkaline and PEM electrolysers are well proven devices with thousands of units in operation, while the solid-oxide electrolyser is as yet unproven. The PEM electrolyser is particularly well suited to highly distributed applications. The alkaline electrolyser currently dominates global production of electrolytic hydrogen.

Alkaline water elecrolysis is the dominating technology today

According to faraday' law, hydrogen production rate of an electrolyzer can be obtained as:

$$n_{H_2} = \frac{\eta_F n_C i_e}{2F} \tag{21}$$

Where:

F: Faraday constant.

i_e: Electrolyzer current.

n_C: The number of electrolyzer cells in series.

η_F: Faraday efficiency.

n_{H2}: Produced hydrogen moles per second.

XII. HYDROGEN STORAGE SYSTEM

One of the hydrogen storage techniques is physical hydogen storage, which involves using tanks to store either compressed hydrogen gas or liquid. The hydrogen storage model based on Eq (22) an it directly calculates the tank pressure using the ration of hydrogen flow to the tank. The produced hydrogen is stored in the tank, whose system dynamic can be compressed as follow [29, 30]:

$$P_b - P_{bi} = z \frac{N_{H_2} R T_b}{M_{H_2} V_b} \tag{22}$$

Where:

M_{H2}: Molar mass of hydrogen.

N_{H2}: Hydrogen moles per second delivered to the storage tank.

P_b: Pressure of tank.

P_{bi}: Initial pressure of the storage tank.

R: Universal gas constant.

T_b: Operating temperature.

V_b: Volume of the tank.

z: Compressibility factor as a function of pressure.

The hydrogen state-of-storage (SHS) is therefore:

$$SHS = \frac{P_b}{P_{b\,max}} \tag{23}$$

Where:

P_b: Pressure of tank.

P_{bmax}: is the maximum Pressure of tank.

XIII. OVERALL POWER MANAGEMENT STRATEGY

A control system was developed to determine when to produce hydrogen and when to convert it back to
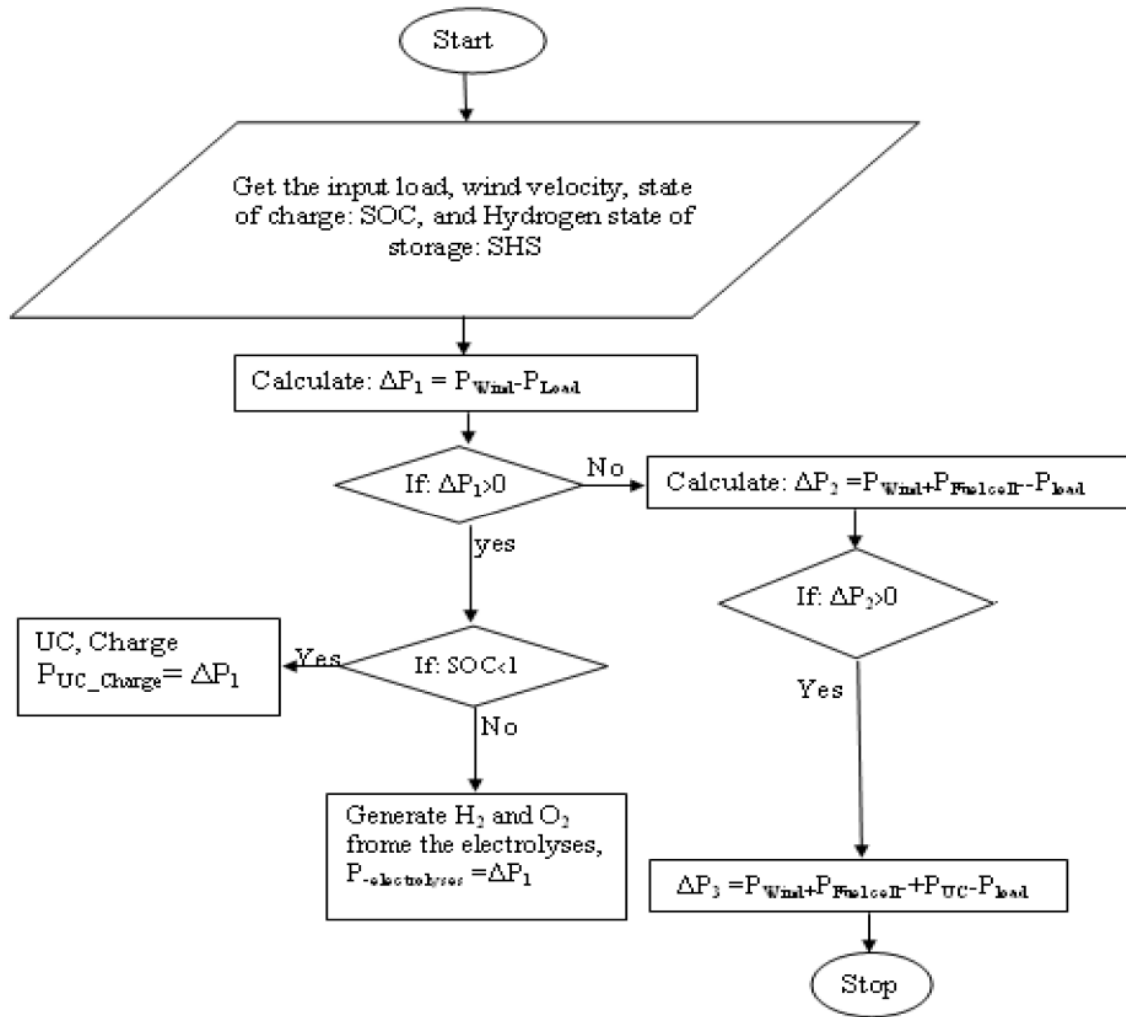
Figure 9: Flow chart of system management.

electricity. The control algorithm is based on the UC' state-of-charge (SOC) and the hydrogen' state-of-storage (SHS). Knowing the load demand, the surplus energy is determined. The surplus energy is used to generate hydrogen from the electrolyzer, which is stored in tanks. At the times when the wind source is unable to supply the load demand, the stored hydrogen is supplied to the fuel cells (FC). The UC bank serves as a short duration power source to meet the excess power that cannot be satisfied by the FC or the wind system.

The flow chart describing the management of the power flow in the proposed system is shown in Figure **9**.

XIV. SIMULATION RESULTS

Based on the component models given earlier, a simulation system for the proposed hybrid energy system has been developed in Matlab/simulink.

The wind speed ranging between 4 and 10m/s with an average value of 7 m/s is presented on the Figure **10**. This sequence is obtained by adding a turbulent component to a slowly varying signal. Respectively.
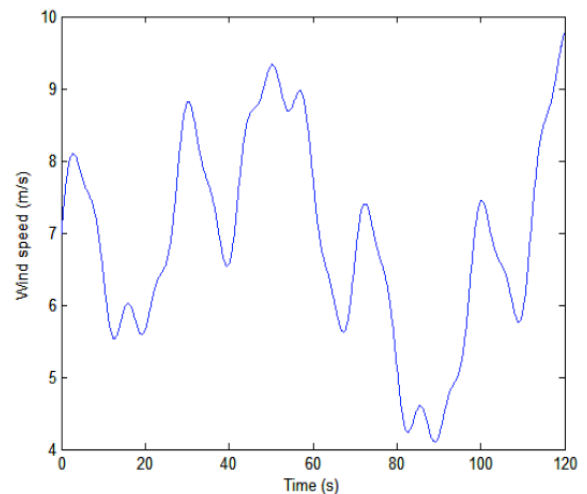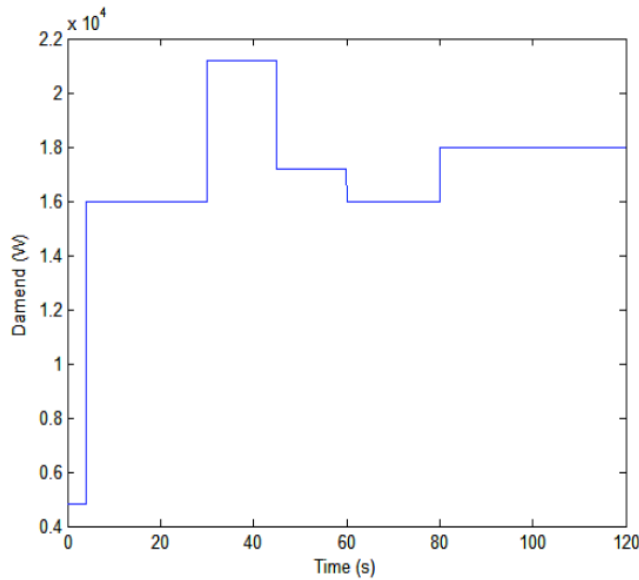

Figure 10: Wind speed.

Figure 11: Load power demand.

The UC state-of-charge (SOC) is given in the Figure **13**.

When the wind generated power from is not sufficient to supply the load demand (for example see Figure **11**, for t=80s to 100s). Under this condition, the fuel cell turns on to supply the power shortage and the UC bank serves as a short duration power source to meet the excess power that cannot be satisfied by the FC or the wind system.
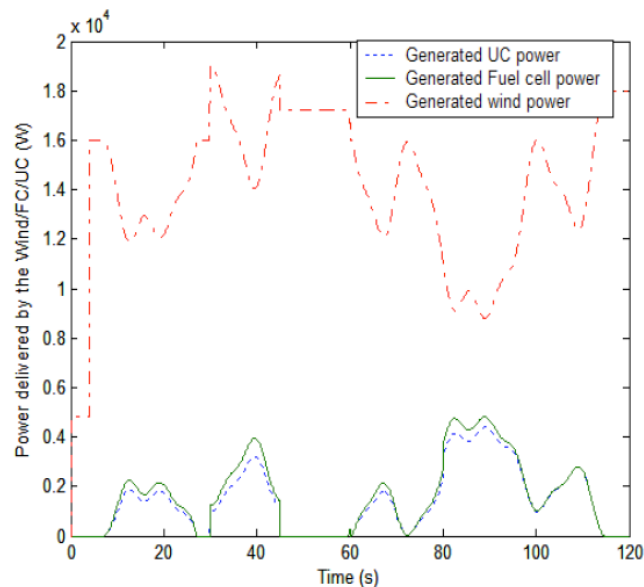

Figure 12: Power delivered to the load side by the Wind/FC/UC hybrid topology.

When, there is the surplus power available for stored (see Figures **11** and **12**, for t=45s to 60s). The control algorithm based on the UC' state-of-charge

(SOC) and the hydrogen' state-of-storage (SHS) is also used to fix the power stored in each system (UC bank and electrolyser system).

The H_2 storage tank pressure varies as H_2 flows in and out. It is apparent that the storage tank pressure will go up when there is excess power available for H_2 generation and will decrease when the FC supplies power to load and consumes H_2. Figure **14** shows the tank pressure variations over the simulation period.
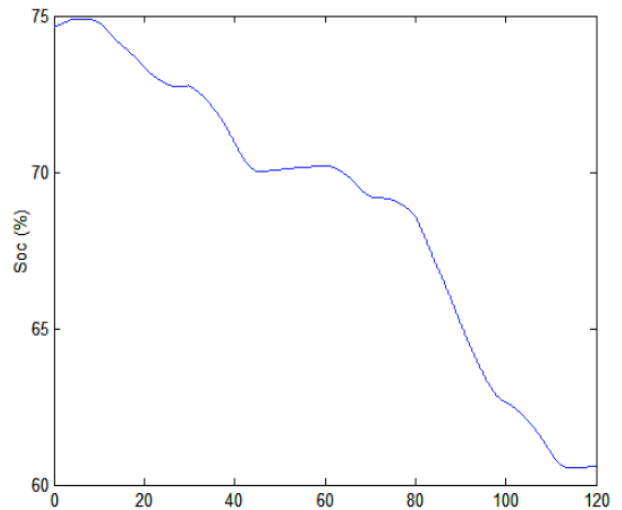

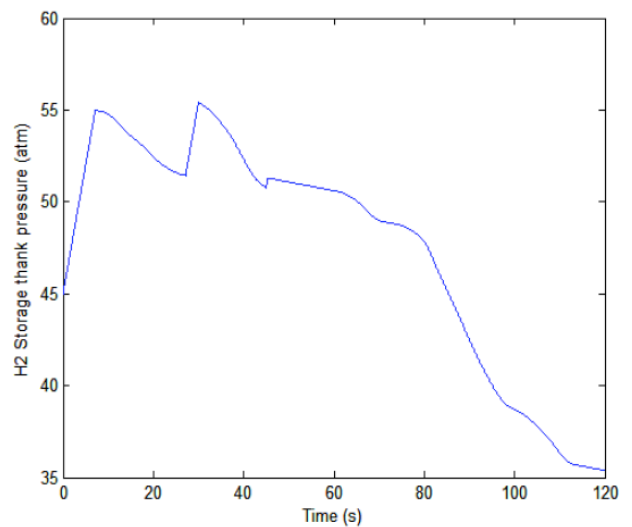**Figure 13:** The state-of-charge (SOC).

Figure 14: The H_2 tank pressure.

Finally, the user power requirement and the power delivered to the load side by the Wind/FC/UC hybrid system are illustrated in Figure **15**.

XV. CONCLUSION

In this paper, a hybrid wind/FC/UC System Performance is proposed; the WECS was modeled
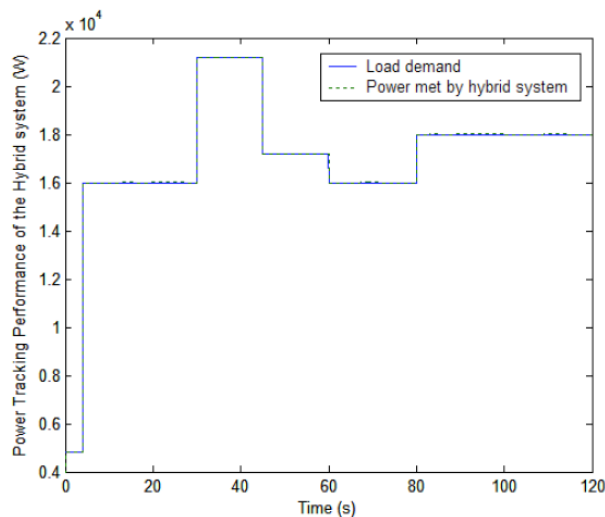
Figure 15: Power tracking performance of the hybrid topology.

using d-q rotor reference frame and the variable speed wind generator maximum power point tracking based on an adaptive Neuro-Fuzzy-Inference-System (ANFIS) was presented.

The results show also the excellent performance of the hybrid topology proposed under variable wind speed and load power requirements, so we can used this system in the non ideal wind speed areas.

REFERENCES

[1] Khan MJ, Iqbal MT. Dynamic modeling and simulation of a small wind fuel cell hybrid energy system. J Renewable Energy 2005; 30(3): 421-39.
http://dx.doi.org/10.1016/j.renene.2004.05.013

[2] De Battista H, Mantz RJ, Garelli F. Power conditioning for a wind hydrogen energy system. J Power Sources 2006; 155(2): 478-86.
http://dx.doi.org/10.1016/j.jpowsour.2005.05.005

[3] Karaki HS, Chedid RB, Ramadhan R. Probabilistic performance assessment of autonomous solar-wind energy conversion system. IEEE Trans Energy Conver 1999; 14(3): 766-72.
http://dx.doi.org/10.1109/60.790949

[4] Deshmukh MK, Deshmukh SS. Modeling of hybrid renewable energy systems. J Renewable Sustainable Energy Rev 2008; 12: 235-49.
http://dx.doi.org/10.1016/j.rser.2006.07.011

[5] Eminoglu U. Modelling and Application of Wind Turbine Generating Systems (WTGS) to. Distribution Systems. In J Renewable Energy 2009; 34: 2474-83.
http://dx.doi.org/10.1016/j.renene.2009.03.026

[6] Meharrar A, Tioursi M, Hatti M, Stambouli AB. A variable speed wind generator maximum power tracking based on adaptive neuro-fuzzy inference system. J Expert Systems Appl 2011; 38: 7659-64.
http://dx.doi.org/10.1016/j.eswa.2010.12.163

[7] El-Sharkh MY, Rahman A, Alam MS. Neural Networks Based Control of Active and Reactive Power of a Stand- alone PEM Fuel Cell Power Plant. Int J Power Sources 2004; (135): 88-94.
http://dx.doi.org/10.1016/j.jpowsour.2004.03.071

[8] High Efficiency fossil power plants (HEFPP) conceptualization Program, Final Report, DE-97FT 34164, Fuel Cell Energy Inc. CT March 1999.

[9] Meharrar A. Modélisation, Optimisation et Contrôle des Systèmes Hybrides: Eolienne/Pile à combustible. Ph.D. dissertation. Faculty of Electrical Engineering, University of Sciences and Technology of Oran, Algeria 2012.

[10] Sakhare A, Davari A, Feliachi A. Fuzzy logic control of fuel cell for stand-alone and grid connection. J Power Sources 2004; 135: 165-76.
http://dx.doi.org/10.1016/j.jpowsour.2004.04.013

[11] Hatti M, Meharrar A, Tioursi M. Power management strategy in the alternative energy photovoltaic/PEM Fuel Cell hybrid system. Renewable Sustainable Energy Rev 2011; 15: 5104-10.
http://dx.doi.org/10.1016/j.rser.2011.07.046

[12] Hofmann Ph, Panopoulos KD. Detailed dynamic Solid Oxide Fuel Cell modeling for electrochemical impedance spectra simulation. J Power Sources 2010; 195: 5320-39.
http://dx.doi.org/10.1016/j.jpowsour.2010.02.046

[13] Sedghisigarchi K, Feliachi A. Dynamic and Transient Analysis of Power Distribution Systems with Fuel Cells Fuel. IEEE Trans Energy Conversion 2004; 19(Pt 1): 423-28.

[14] Padulles J, Ault GW. McDonald JR. An integrated SOFC plant dynamic model for power systems simulation. J Power Sources 2000; 86: 495-500.
http://dx.doi.org/10.1016/S0378-7753(99)00430-9

[15] Xiao W, Xin-Jian Z, Guang-Yi C, Heng-Yong Tu. Predictive control of SOFC based on a GA-RBF neural network model. J Power Sources 2008; 179: 232-39.
http://dx.doi.org/10.1016/j.jpowsour.2007.12.036

[16] Uzunoglua M, Alama MS. Load sharing using fuzzy logic control in a fuel cell/ultracapacitor hybrid vehicle M.C. Kisacikoglua. Int J Hydrogen Energy 2009; 4: 1497-507.

[17] Hauer K-H. Analysis tool for fuel cell vehicle hardware and software (controls) with an application to fuel economy comparisons of alternative system designs. Ph.D. dissertation, Dept. Transportation Technology and Policy, Univ. California, Davis 2001.

[18] El-Sharkh MY, Rahman A, Alam MS, Byrne PC, Sakla AA, Thomas T. A dynamic model for a stand-alone PEM fuel cell power plant for residential applications. J Power Sources 2004; 138(1-2): 199-204.
http://dx.doi.org/10.1016/j.jpowsour.2004.06.037

[19] Kirubakaran A, Jain S, Nema RK. The PEM Fuel Cell System with DC/DC Boost Converter: Design, Modeling and Simulation. Int J Recent Trends Eng 2009; 1(3).

[20] Mohan N, Undeland TM, Robbins WP. Power Electronics Converters, Applications and Design. J Wiley & Sons 2001.

[21] Wang YM, Taha MS, Elhag. An adaptive neuro- fuzzy inference system for bridge risk assessment. Int J Expert Systems Appl 2008; 34(3): 3099-106.
http://dx.doi.org/10.1016/j.eswa.2007.06.026

[22] Candusso D, Rulličre EE, Toutain E. A Fuel Cell Hybrid Power Source for a Small Electric Vehicle. Energy Renewable: Power Eng 2001; 85-92.

[23] Kisacikoglu MC, Uzunoglu MC, Alam M. Load sharing usingfuzzy logic control in a fuel cell/ultracapacitor hybrid vehicle. Int J Hydrogen Energy 2009; 34: 497-507.
http://dx.doi.org/10.1016/j.ijhydene.2008.11.035

[24] Zhang X, Mi C, Masrur A, Daniszewski D. Wavelet based power management of hybrid electric vehicles with multiple onboard power sources. J Power Sources 2008; 185: 1533-43.
http://dx.doi.org/10.1016/j.jpowsour.2008.08.046

[25] Spyker RL, Nelms RM. Analysis of double-layer capacitors supplying constant power loads. IEEE Trans Aerosp Electron Syst 2000; 36(4): 1439-43.
http://dx.doi.org/10.1109/7.892696

[26]   Spyker RL, Nelms RM. Classical equivalent circuit Parameters for a Double-Layer Capacitor. IEEE Trans Aerospace Electr Syst 2000; 36(3): 829-36.

[27]   Kotsopoulos A, Duarte JL, Hendrix M. A converter to interface ultra-capacitor energy storage to a fuel cell system. Proceedings 2004 IEEE Int Symposium Indust Electron 2004; 2: 827-32.
http://dx.doi.org/10.1109/ISIE.2004.1571920

[28]   Wenzhong G. IEEE Trans Veh Technol 2000; 54(3): 846-55.

[29]   Haluk G. Dynamic Modeling of a Proton Exchange Membrane (PEM) Electrolyser. Int J Hydrogen Energy 2006; 31: 29-38.
http://dx.doi.org/10.1016/j.ijhydene.2005.04.001

[30]   Onar OC, Uzunoglu M, Alam MS. Dynamic modeling, design and simulation of a wind/fuel cell / ultracapacitor based hybrid power generation system. J Power Sources 2006; 161(1): 707-22.
http://dx.doi.org/10.1016/j.jpowsour.2006.03.055